Parametric Decay Wave Observation in HFS X-Mode Injection in QUEST*)

Shinichiro KOJIMA, Hatem ELSERAFY[1)], Kazuaki HANADA[1)], Hiroshi IDEI[1)], Ryuya IKEZOE[1)], Yoshihiko NAGASHIMA[1)], Makoto HASEGAWA[1)], Takumi ONCHI[1)], Kengoh KURODA[1)], Kazuo NAKAMURA[1)], Takahiro MURAKAMI, Masaharu FUKUYAMA, Ryoya KATO, Ryota YONEDA[2)], Masayuki ONO[3)], Akira EJIRI[4)], Yuichi TAKASE[4)] and Sadayoshi MURAKAMI[5)]

Interdisciplinary Graduate School of Engineering Sciences, Kyushu University, Kasuga, Fukuoka 816-8580, Japan
[1)]*Research Institute for Applied Mechanics, Kyushu University, Kasuga, Fukuoka 816-8580, Japan*
[2)]*Department of Physics & Astronomy, University of California Los Angeles, Los Angeles, CA 90095, USA*
[3)]*Princeton Plasma Physics Laboratory, Princeton, NJ 08540, USA*
[4)]*Graduate School of Frontier Sciences, The University of Tokyo, Kashiwa, Tokyo 277-8561 Japan*
[5)]*Graduate School of Engineering, Kyoto University, Kyoto 615-8540, Japan*

(Received 5 December 2019 / Accepted 5 July 2020)

The parametric decay wave (PDW) caused by three-wave parametric decay process was measured in a plasma-injecting X-mode electron cyclotron wave (ECW) from the high field side (HFS) of the Q-shu University Experimental Steady-State Spherical Tokamak (QUEST). The intensity of the low-frequency PDW on the HFS X-mode injection was significantly enhanced over the O-mode ECW injection from the low field side (LFS), where the mode conversion to electron Bernstein wave (EBW) was not expected. As the comparison was executed using plasmas with the same magnetic field and injection power, the wave injection method was considered as the primary cause of the difference in the PDW excitation. The frequency range of the low-frequency PDW was consistent with that of the lower hybrid wave (LHW) range, which was expected to be excited during the mode conversion to EBW. The low-frequency PDW intensity evolved in response to the plasma density, plasma current and injection power. This observation suggests that the low-frequency PDW intensity is a reliable indicator for the efficient mode conversion to EBW.

Keywords: electron Bernstein wave, parametric decay instability, X-B mode conversion, high field side injection, QUEST

DOI: 10.1585/pfr.15.2402063

1. Introduction

Spherical tokamaks (STs) are promising candidates for future fusion power plants owing to greater stability in obtaining high beta plasma when compared to conventional tokamaks. Inductive current drive by ohmic heating is the most common method of plasma production, but its capability is insufficient for an ST because of the small cross section of the center solenoid (CS). Electron cyclotron heating/current drive (ECH/CD) have been demonstrated to heat and noninductively drive plasma current in STs as in LATE [1] and Q-shu University Experimental Steady-State Spherical Tokamak (QUEST) [2, 3]. However, the presence of a density limit facing the propagating electron cyclotron wave (ECW), which is a type of an electromagnetic wave, prevents the production of high-density plasmas that are required to obtain a higher beta regime for attractive fusion reactors. On the other hand, an electron Bernstein wave (EBW), an electrostatic wave has no density limit and can, therefore, propagate even in high-density plasma and efficiently transfer its power to plasmas. A method for EBW heating in STs was first proposed by Cairns *et al.* [4]. Three types of mode conversion processes from ECW to EBW have been established. The method known as the O-X-B mode conversion involves excitation of EBW by injecting from the low field side (LFS) and double mode conversion from ordinary mode (O-mode) to extraordinary mode (X-mode) and from X-mode to electron Bernstein mode (B-mode) at upper hybrid resonance (UHR), as demonstrated by LATE [5], TCV [6], W7-AS [7], and LHD [8, 9]. However, the double mode conversion in this method indicate its complexity and difficulty to apply. The second established method, X-B mode conversion from the LFS, includes mode conversion to EBW from X-mode LFS injection, and was demonstrated in TST-2 [10]. In the X-B mode conversion from the LFS, a steep density gradient is required to obtain high conversion efficiency, so it is difficult to apply to achieve plasma

author's e-mail: kojima@triam.kyushu-u.ac.jp
*) This article is based on the presentation at the 28th International Toki Conference on Plasma and Fusion Research (ITC28).

current start-up. The third established method of mode conversion, X-B mode conversion from the high field side (HFS), shows promise for efficient conversion from ECW to EBW. As indicated by the GENRAY [11] calculation, X-B mode conversion from the HFS is possible without a complicated optimization of the wave injection angle [12]. This method has been investigated in COMPASS-D [13], WT-3 [14], LHD [15], Versator II [16] and QUEST [17]. In LHD, the direct launching of the X-mode from the HFS has been executed to utilize a merit of helical magnetic field [15]. In previous experiments, most of these devices utilized a mirror on the CS surface with the exception of QUEST [17]. However, it is difficult to confirm whether the externally injected wave has significant purity of the X-mode after the reflection at the mirror, and they did not perform a direct comparison of an ECW injection from the HFS and from the LFS as in the present experiment.

In all the three methods described above, the observation of mode conversion to EBW is critical. In case of O-X-B mode conversion from LFS injection, the monitoring stray radiation to search O-X-B mode conversion window is a very helpful method to effectively excite EBW [18]. However, collateral observation of the mode conversion for any mode conversion method should be accomplished. The observation of parametric decay instability (PDI), also known as three-wave parametric decay process is a good candidate for collateral observation of mode conversion regardless of a certain mode conversion method. In Versator II, parametric decay waves (PDWs) of the upper hybrid wave and lower hybrid wave (LHW) frequency ranges were observed during the X-mode launching from the HFS [16]. The large amplitude of the electric field in the UHR layer, which allowed for the production of PDWs, may provide collateral evidence indicating the occurrence of mode conversion. In this study, to investigate the possibility of observing the collateral evidence of mode conversion to EBW, the low-frequency PDW intensity in plasmas for the X-B conversion from the HFS and the conventional ECW injection from the LFS (where mode conversion to EBW was not expected) were measured by inserting a probe.

2. Experimental Setup

The experiment was conducted in QUEST, which is a mid-size ST device with an aspect ratio of 1.6, major radius $R = 640$ mm, minor radius $a = 400$ mm, and CS cover radius $r_{cs} = 200$ mm. The maximum toroidal magnetic field was 0.25 T at $R = 640$ mm with a toroidal coil current of 50 kA. The equipped radio frequency (RF) sources were 2.45 GHz and 8.2 GHz klystrons and a 28 GHz gyrotron for the ECW. We installed new transmission lines in the vacuum vessel for the ECW injection from the HFS [19]. Two 20 kW/8.2 GHz klystrons were connected to each main transmission line which is constructed of atmospheric RG-50 waveguides. To transmit the wave through the vacuum vessel to the HFS X-mode injection point, we installed vacuum windows, and copper waveguides, in the top and bottom sides, as shown in Fig. 1 (a). The vacuum windows were in the HFS of the ECR layer and were not equipped with a water-cooling channel in this study, so discharge time was restricted to short durations. We inserted a switch after the main transmission line so that the direction of the ECW injection could be changed from LFS injection to HFS injection easily. To avoid arcing and breakdown inside the transmission lines placed near the ECR layer, SF_6 gas was filled inside transmission lines from the klystrons

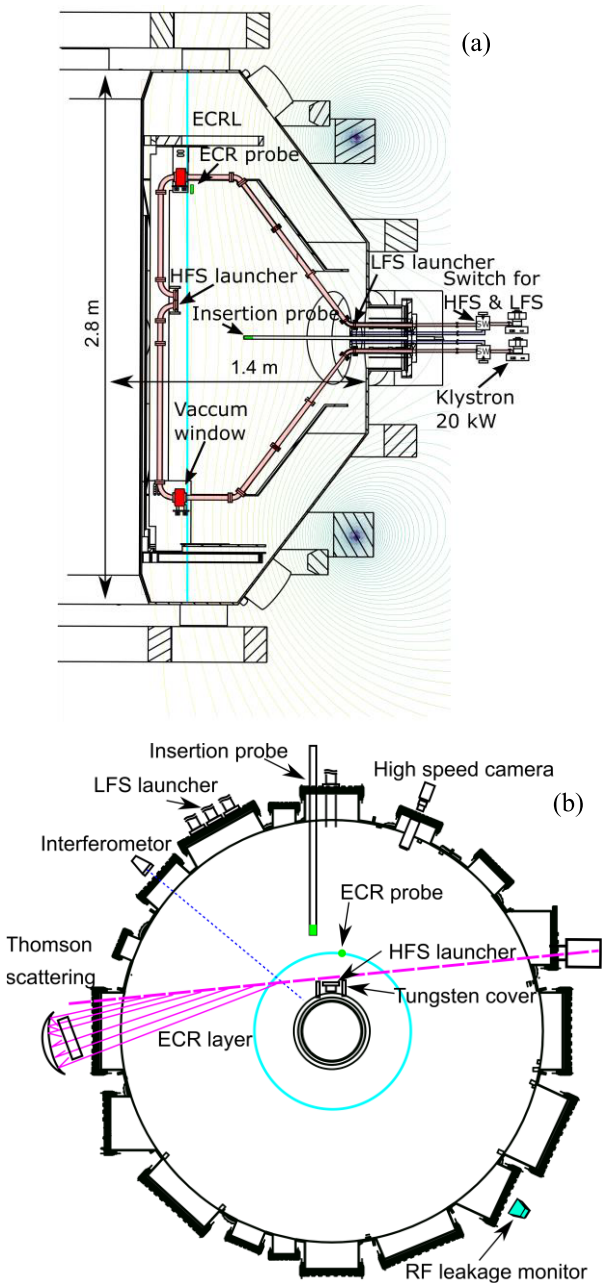

Fig. 1 Experimental setup showing both the (a) poloidal and (b) top views. (a) Poloidal view showing the locations of the HFS launcher, LFS launcher, ECR probe, and insertion probe in the vacuum vessel. The vertical light blue line indicates the position of fundamental ECR layer. (b) Top view of the QUEST showing each equipment. The RF leak detector was located outside the vacuum vessel.

to the vacuum windows. To prevent damage to the windows by heat, the maximum discharge time was limited to 110 msec in the HFS injection. The LFS injection antenna launched O-mode, and the HFS injection antenna launched X-mode after adjusting the TE_{10} mode waveguides polarization. The surface of the HFS injection antenna was located at R = 323 mm. To protect the copper waveguides from plasma contact, we covered them with stainless steel SUS304 and installed two tungsten limiters antenna terminals. The tip of the tungsten limiter was located at R = 363 mm. The toroidal coil current was set to 40 kA. The fundamental ECR layer for the 8.2 GHz ECW was located at R = 437 mm.

A Thomson scattering system was equipped to measure the T_e and n_e profiles at R = 340, 468, 634, 774, 934 and 1080 mm. The yttrium aluminum garnet (YAG) laser required nearly 100 msec to charge in the capacitor bank. Owing to inadequate time resolution, the measurement time was set at 2 msec and 102 msec. A 75 GHz RF interferometer was injected in the direction of the center stack. The RF wave of the interferometer was reflected by the surface of the center stack and detected by the antenna located at the same observation port. The line-integrated density shows the integrated density profile along the R direction on the midplane.

The mode conversion efficiency from ECW to EBW is difficult to measure directly. However, when the mode conversion occurs, the RF power absorption should increase because EBW is efficiently absorbed, even in low-temperature plasmas. The RF absorption for the input power was indicated by comparing the voltage of the RF leakage monitor (RLM) signal in the cases of RF injection to plasma and to vacuum. The RLM was installed outside of the vacuum vessel, as shown in Fig. 1 (b).

We prepared two electrostatic probes to measure the low-frequency PDW. The electron cyclotron resonance (ECR) probe, was placed near the ECR layer at R = 465 mm, Z = 820 mm so that it could be reference signal to confirm the reproducibility, and the insertion probe was inserted into the plasma in the range of R = 400 - 900 mm, Z = 0 mm so that it could directly measure PDWs around the UHR layer. It was anticipated that the insertion probe interferes with the laser path of the Thomson scattering system, so it was pulled back to R = 1150 mm during the Thomson measurement. A simultaneous measurement by the insertion probe around UHR layer and the Thomson scattering was therefore not possible. The exposed electrostatic probe pins were tungsten with diameter = 1 mm and length = 1.6 mm. The insertion probe was supported by stainless steel SUS304. The insertion probe (except the pins) were covered by alumina ceramic with a length of 960 mm. The ECR probe except the pins was installed behind waveguides cover. In the experiment using the insertion probe, the discharge duration was limited to 10 msec to avoid producing cracks in the alumina ceramic cover. The probes were directly connected to an oscilloscope with a −20 dB attenuator. The oscilloscope was type HDO8038A, which we set to a frequency band of 350 MHz and a sampling rate of 1.25 GS/sec.

3. Experimental Results of PDW Observation

In this experiment, the plasma startup was performed noninductively. The ECW injection was implemented using two methods: X-mode injection perpendicular to the magnetic field from the HFS, which was expected to result in an efficient mode conversion into EBW at the UHR layer, and O-mode injection using a phased array antenna [20], which was not expected to perform mode conversion. The phased array antenna requires eight klystrons to be complete, but only two klystrons were available for this experiment; therefore, the complete ECW focusing and control of injection angle was difficult. This indicates that the potential for the O-X-B and X-B mode conversion methods from the LFS as described above cannot be expected. We regarded the LFS injection with no EBW mode conversion as a good reference compared with the HFS injection. Improved plasma parameters in the HFS injection compared to the LFS injection were reported previously [19]. In this paper, we carefully produced discharges with same plasma operation in both HFS and LFS injections; therefore, the parameters are different from the our previous report [19]. The line-integrated density in both injections in the last part of the discharge was similar, as shown in Figs. 2 (c: H, L), but significant differences in I_p and RLM signal, shown in Figs. 2 (b, e: H, L), were observed. These signals indicate a greater difference in RF absorption between the HFS and LFS injection as previously reported [19]. The density is the most important parameter for inducing EBW mode conversion.

In order to measure the collateral evidence of the EBW excitation, the PDW was measured with the insertion probe in reproducible 10 msec duration plasmas to avoid significant damage to the probe from the heat flux of the plasma. To check the impact of the probe insertion, each plasma parameters in the different insertion probe positions are shown in Fig. 2. A slight impact of the measured plasma parameters was observed in the discharge with deep probe insertion. In the initial phase of the discharge of the HFS injection, both the plasma current and the line-integrated density were impacted, but this timing of signals shows poor reproducibility. In fact, the timing of the peak of I_p fluctuated within a few msec. After this, all the signals were constant up to 10 msec and were less impacted by the insertion of the probe. Video of plasma with and without inserting the probe in the HFS injection were recorded, as shown in Fig. 3. A slightly bright area that was induced by the probe was observed, but the impact was located on the pipe that supports the probe and was negligible on the probe head. Modification of the magnetic flux surface caused by the difference in I_p should also be dis-

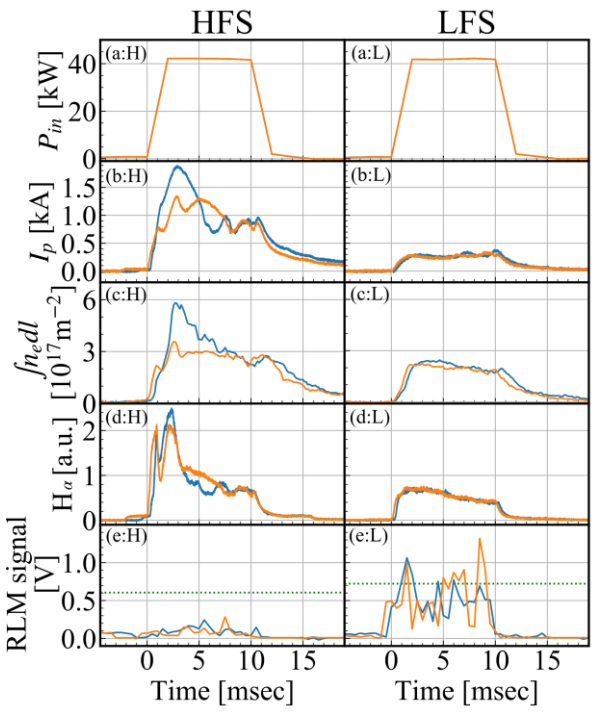

Fig. 2 Time evolution of (a: H, L) RF input power, (b: H, L) plasma current, (c: H, L) line integrated density, (d: H, L) H α intensity, and (e: H, L) RLM signal. (a - e: H) X-mode HFS injection. (a - e: L) O-mode LFS injection. Each insertion probe position at R = 900 mm are drawn by solid blue lines (HFS: #39339, LFS: #39355). Each insertion probe position at UHR layer are drawn by solid orange lines (HFS: R = 550 mm #39345, LFS: R = 600 mm #39358). In (e: H, L), a green dotted line shows the maximum value of RLM signal in no plasma with same input power.

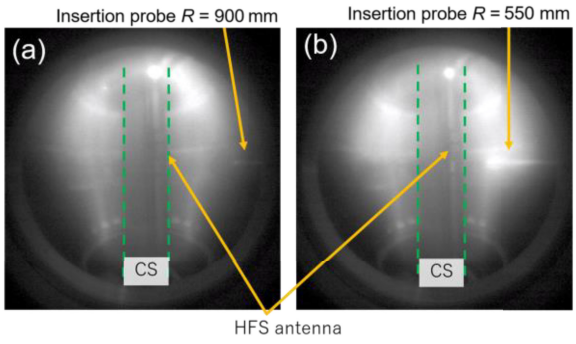

Fig. 3 The visible light video images in the HFS injection at 5 msec. (a) Plasma without insertion probe (R = 900 mm). (b) Plasma with insertion probe (R = 550 mm).

cussed. Most of the observed plasma current was relevant to the pressure driven current in the open magnetic flux surface [21] estimated by the T_e and n_e profiles as measured using Thomson scattering. No evidence for the formation of a closed flux surface was observed in either the video images or the magnetic signals. Therefore, the difference in I_p did not play a role in the modification of the magnetic surface. A slight impact of the deep probe insertion on the plasma parameters is supportive evidence for the condition

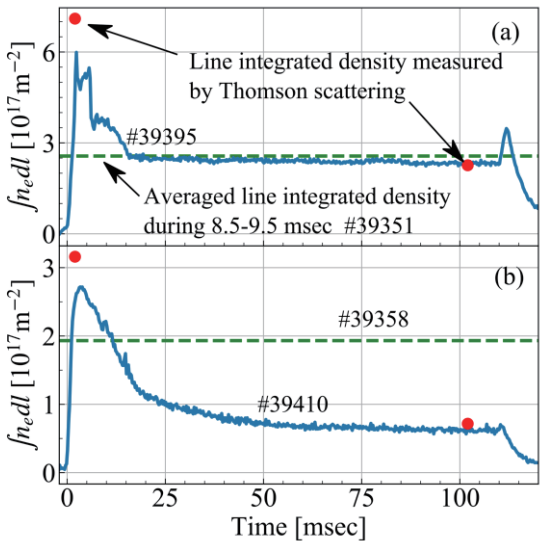

Fig. 4 Time evolution of the line-integrated density 110 msec discharge for (a) the HFS injection (#39395) and (b) the LFS injection (#39410) are drawn by the blue lines. The line-integrated densities calculated on ne profiles measured with Thomson scattering were marked by the red points. The green dot lines show averaged line-integrated density during 8.5 - 9.5 msec in 10 msec discharges (HFS: #39351, LFS: #39358).

of no closed flux surface because such a deep insertion of probes into a closed flux surface would have broken the closed flux surface. If closed flux surface were formed, the probe insertion would interrupt particles on same flux surface surrounding the magnetic axis causing a large impact on the plasma parameters [22].

To estimate the UHR layer location and the PDW frequency for the PDW measurement, we estimated the n_e profiles in both injections of PDW measurement from the measured n_e profiles with the Thomson scattering. The time evolution of the measured line-integrated electron density and the calculated line-integrated electron density based on Thomson scattering measurement, and the averaged line-integrated electron density during 8.5 - 9.5 msec on the PDW measurement were shown in Fig. 4. In HFS injection, the averaged line-integrated electron density during 8.5 - 9.5 msec on PDW measurement and the line-integrated electron density after 15 msec on Thomson scattering measurement had similar values. We assumed that the formation of the n_e profile should be the same in both measurements to estimate the n_e profiles on PDW measurement. The n_e profiles measured with Thomson scattering at 102 msec were much more reliable than those at 2 msec. The n_e profiles at the PDW measurement were estimated by multiplying the n_e profiles at 102 msec by each factor (F_{HFS}: 1.1, F_{LFS}: 2.7) to adjust the line-integrated density measured by Thomson scattering to be consistent with the line-integrated density measured by the interferometer during the PDW measurement. The estimated n_e profiles at the PDW measurement and the measured n_e profiles based on the Thomson scattering mea-

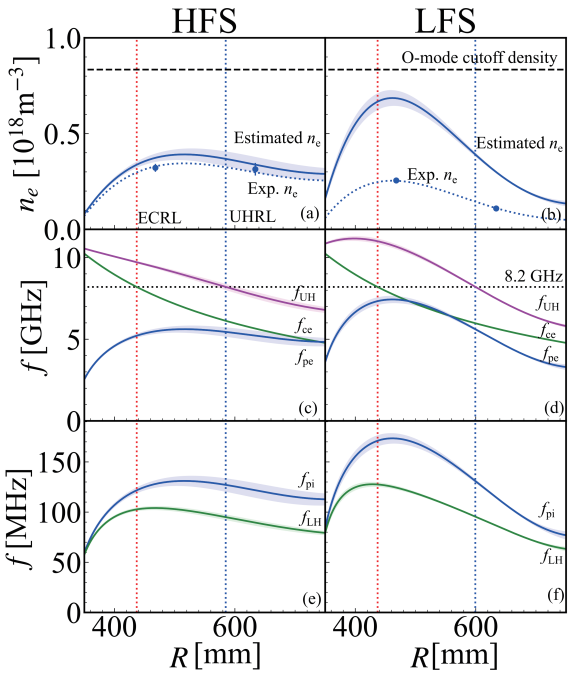

Fig. 5 (a, b) The solid blue lines show the estimated ne profiles during 8.5 - 9.5 msec for HFS (#39351) and LFS (#39358) injections. The dotted blue lines show the obtained ne profiles by the Thomson scattering measurement (HFS: #39395, LFS: #39410). The black dash line shows the O-mode cutoff density. (c - f) The calculated frequencies that depend on the estimated electron density distribution. The red, blue and dotted black lines show the locations of the ECR layer, UHR layer and the frequency of the injected ECW wave. (a, c, e) The HFS injection. (b, d, f) The LFS injection. (c, d) Frequency of GHz order in the R direction. The solid blue, green, and magenta lines show the electron plasma frequency, the electron cyclotron frequency, and the upper hybrid frequency, respectively. (e, f) Frequency of MHz order in the R direction. The solid blue and green lines show the ion plasma frequency and the lower hybrid frequency, respectively.

surement were shown in Figs. 5 (a, b). The O-mode cutoff density at 8.2 GHz was 8.7×10^{17} m^{-3}. In both injections, the over-dense regions were not observed on the estimated and measured n_e profiles. This means that it was not possible to obtain the O-X-B mode conversion from the LFS injection. The broad n_e profile was observed in the HFS injection, and the narrow peaked n_e profile was obtained in the LFS injection. According to the estimated n_e profiles, the characteristic frequencies of interest were calculated, as shown in Figs. 5 (c - f). The UHR layer of the HFS and LFS injections were located at R = 575 mm and R = 600 mm, respectively. In the experiment, the insertion probe surveyed in the range of R = 400 - 900 mm. The discharges on the probe, inserted on R = 550 mm and R = 600 mm, were selected to analyze the PDW for the HFS and LFS injections, respectively.

The spectra by the fast Fourier transform (FFT) analysis were obtained from the measured potential signals with

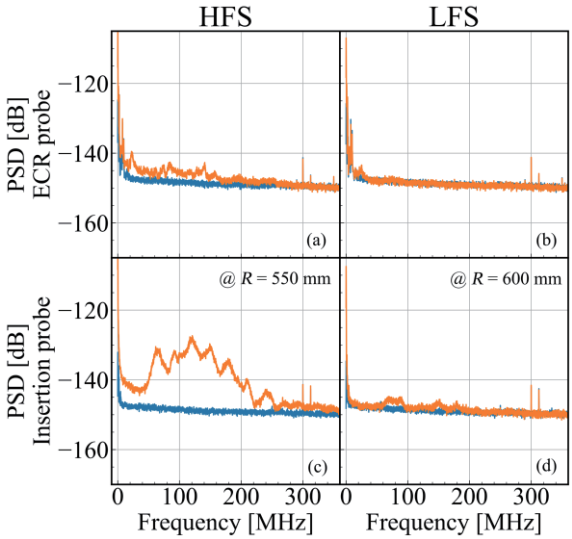

Fig. 6 Power spectral densities (PSDs) of (a, b) the ECR probe and (c, d) the insertion probe around the UHR layer (HFS: R = 550 mm, LFS: R = 600 mm) on (a, c) HFS injection (#39351) and (b, d) LFS injection (#39358). The blue lines are PSDs before RF injection. The orange lines are PSDs in the time range of 8.5 - 9.5 msec.

the ECR probe and the insertion probe around the UHR layer in the plasma with the HFS and LFS injections, as shown in Fig. 6. As shown in Fig. 6 (c), the clear amplitude enhancement in the broad frequency range up to 250 MHz was observed by the insertion probe. In Fig. 6 (a), the increased amplitude in the broad frequency was also observed, but the increment of amplitude by the insertion probe was much larger than that by the ECR probe. It may imply that the spectra were excited around the UHR layer and propagated to the ECR probe. On the other hand, the amplitude enhancement such as the one obtained in HFS injection was not observed in LFS injection. The clear difference is observable even in similar plasma conditions and it appears to depend on the different methods of the ECW injection.

The low-frequency PDW by the three-wave parametric decay process induced by EBW excitation should appear around the LHW frequency. The LHW frequency was theoretically calculated by using Eq. 1 and is illustrated in Figs. 5 (e, f):

$$\omega_{LH} = \frac{1}{\sqrt{\frac{1}{\Omega_e \Omega_i} + \frac{1}{\omega_{pi}{}^2}}}, \tag{1}$$

where Ω_e, Ω_i, and ω_{pi} are the angular frequencies of the electron cyclotron frequency, the ion cyclotron frequency, and the ion plasma frequency, respectively. Calculations based on Eq. 1 show that the LHW frequency was ≅ 95 ± 3 MHz at the UHR layer (R = 575 mm) in the plasma with the HFS injection, and ≅ 95 ± 1 MHz at the UHR layer (R = 600 mm) in the plasma with the LFS injection. The PSD denoted in Fig. 6 (c) displays a strong spectrum of around 80 - 120 MHz showing PDW and a spread in the

range of 40 - 240 MHz in the X-mode HFS injection. The actual low-frequency PDW frequency should be spread to the higher side from LHW frequency by the effect of ion temperature [23]. Frequencies lower than the LHW frequency might indicate the propagation of low-frequency PDW which was generated in lower densities on the UHR layer. Each peak of spectra appeared on each ≅ 30 MHz from 60 MHz to 240 MHz. The propagation of these peaks of spectra was observed however, the identification of each wave is difficult by only FFT frequency analysis. On the other hand, few PSDs showing PDW were observed in the O-mode LFS injection as shown in Fig. 6 (d), due to the lack of no mode conversion through O-X-B and X-B as indicated by their n_e profiles. The clear difference of the PSDs between the injection methods is attributed to the mode conversion efficiency. The observed broadening of the PSD in X-mode HFS injection is relevant to the previous observation of the PDW spectrum in Versator II [16]. In this study, the broadening of the spectrum achieved the second harmonic frequency (190 - 240 MHz); however, the second peak was obscured. This may be caused by the difference in low-frequency PDW (≅ 400 MHz in Versator II and ≅ 95 MHz in QUEST). The gap between fundamental and second harmonics of PDW may be buried by the frequency broadening. It is unclear whether the presence of second harmonic frequency is caused by wave excitation at the resonance or by the sheath on the surface of the probe [16, 24].

As shown in Fig. 7, the averaged PSD magnitude of the broadening of the low-frequency PDW from 90 MHz to 110 MHz around the UHR layer showed similar time-dependency to RF power injection and discharge time. The time evolution of the averaged amplitude spectra does not show accurate that of the PDW intensity because the n_e profile always changes, but the possibility of maintained EBW excitation for the entirety of the discharge in the X-mode HFS injection. The PDW measurement is a promising candidate investigating the mode conversion to EBW.

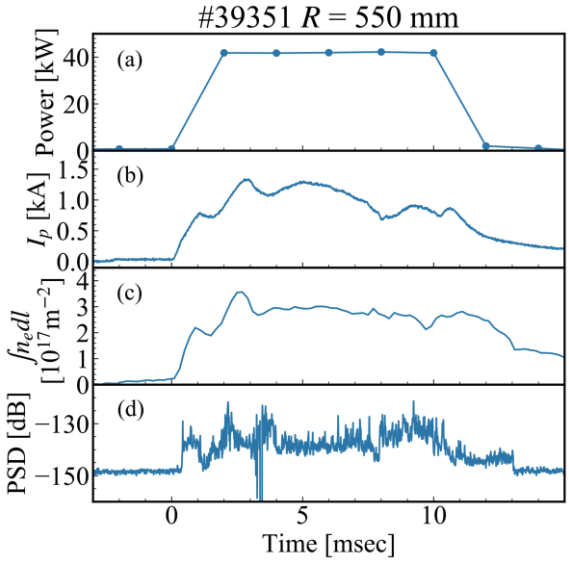

Fig. 7 Time evolution of (a) RF power (time resolution 2 msec), (b) plasma current, (c) line integrated density and (d) the averaged FFT spectrums for 90 - 110 MHz range on the insertion probe.

4. Summary

EBW heating with current drive is one of the suitable actuators to improve the performance of ST devices. In this work, we set up an antenna system in the vacuum vessel to execute the X-B mode conversion using the HFS X-mode injection. The results were compared with those of the plasmas produced by the LFS O-mode injection, which was not expected to cause mode conversion using the same equipment on the same experimental day. The low-frequency PDW spectrum could be obtained for a probe around the UHR layer. A clear difference in the PSD magnitudes of low-frequency PDW was observed while comparing X-mode HFS injection and O-mode LFS injection. The PDW measurement led to a better understanding of the mode conversion to EBW.

Acknowledgments

The authors are grateful to the technical staff of the QUEST group for their helpful support. This work was supported by a Grant-in-Aid for JSPS Fellows (KAKENHI grant numbers 16H02441, 24656559 and 19J12290) and the NIFS Collaboration Research Program (NIFS05KUTRO14, NIFS13KUTR093, NIFS13KUTR085 and NIFS19KUTR136).

[1] M. Uchida *et al.*, J. Plasma Fusion Res. **80**, 83 (2004).
[2] K. Hanada *et al.*, Plasma Sci. Technol. **13**, 307 (2011).
[3] H. Idei *et al.*, Nucl. Fusion **57**, 126045 (2017).
[4] R.A. Cairns and C.N. Lashmore-Davies, Phys. Plasmas **7**, 4126 (2000).
[5] M. Uchida *et al.*, EPJ Web Conf. **87**, EX/P6-18 (2015).
[6] A. Pochelon *et al.*, Nucl. Fusion **47**, 1552 (2007).
[7] H.P. Laqua *et al.*, Phys. Rev. Lett. **90**, 075003 (2003).
[8] H. Igami *et al.*, EPJ Web Conf. **32**, 02006 (2012).
[9] H. Igami *et al.*, EPJ Web Conf. **203**, 02001 (2019).
[10] S. Shiraiwa *et al.*, Phys. Rev. Lett. **96**, 185003 (2006).
[11] A.P. Smirnov *et al.*, Bull Amer. Phys. Soc. **39**, 1626 (1994).
[12] R. Yoneda *et al.*, Plasma Fusion Res. **13**, 3402115 (2018).
[13] V. Shevchenko *et al.*, Phys. Rev. Lett. **89**, 265005 (2002).
[14] T. Maekawa *et al.*, Phys. Rev. Lett. **86**, 3783 (2001).
[15] H. Igami *et al.*, Nucl. Fusion **49**, 115005 (2009).
[16] F.S. McDermott *et al.*, Phys. Fluids **25**, 1488 (1982).
[17] H. Elserafy *et al.*, Plasma Fusion Res. **14**, 1205038 (2019).
[18] H. Igami *et al.*, Rev. Sci. Instrum. **77**, 10E931 (2006).
[19] H. Elserafy *et al.*, Plasma Phys. Control. Fusion **62**, 035018 (2020).
[20] H. Idei *et al.*, Proc. 23rd IAEA FEC IAEA-CN-18, EXW/P7-31 (2010).
[21] T. Yoshinaga *et al.*, Phys. Rev. Lett. **96**, 125005 (2006).
[22] M. Ishiguro *et al.*, Phys. Plasmas **19**, 062508 (2012).
[23] A.T. Lin and C.C. Lin, Phys. Rev. Lett. **47**, 98 (1981).
[24] A.J. Cohen and G. Bekefi, Phys. Fluids **14**, 1512 (1971).